

## Fine Structure in the Energy Region of the Isoscalar Giant Quadrupole Resonance: Characteristic Scales from a Wavelet Analysis

A. Shevchenko,<sup>1</sup> J. Carter,<sup>2</sup> R. W. Fearick,<sup>3</sup> S. V. Förtsch,<sup>4</sup> H. Fujita,<sup>2</sup> Y. Fujita,<sup>5</sup> Y. Kalmykov,<sup>1</sup> D. Lacroix,<sup>6</sup> J. J. Lawrie,<sup>4</sup> P. von Neumann-Cosel,<sup>1,\*</sup> R. Neveling,<sup>4</sup> V. Yu. Ponomarev,<sup>1,†</sup> A. Richter,<sup>1</sup> E. Sideras-Haddad,<sup>2</sup> F. D. Smit,<sup>4</sup> and J. Wambach<sup>1</sup>

<sup>1</sup>*Institut für Kernphysik, Technische Universität Darmstadt, D-64289 Darmstadt, Germany*

<sup>2</sup>*School of Physics, University of the Witwatersrand, PO Wits, Johannesburg 2050, South Africa*

<sup>3</sup>*Physics Department, University of Cape Town, Rondebosch 7700, South Africa*

<sup>4</sup>*iThemba LABS, PO Box 722, Somerset West 7129, South Africa*

<sup>5</sup>*Department of Physics, Osaka University, Toyonaka, Osaka 560-0043, Japan*

<sup>6</sup>*LPC/ISMRA, F-14050 Caen, France*

(Received 1 June 2004; published 15 September 2004)

Fine structure in the energy region of the isoscalar giant quadrupole resonance in nuclei is observed in high-resolution proton scattering experiments at iThemba LABS over a wide mass range. A novel method based on wavelet transforms is introduced for the extraction of scales characterizing the fine structure. A comparison with microscopic model calculations including two-particle two-hole (2p2h) degrees of freedom identifies the coupling to surface vibrations as the main source of the observed scales. A generic pattern is also found for the stochastic coupling to the background of the more complex states.

DOI: 10.1103/PhysRevLett.93.122501

PACS numbers: 24.30.Cz, 21.60.Jz, 25.40.Ep, 27.80.+w

The decay of giant resonances in nuclei is a prime example of how a well-ordered collective excitation dissolves into disordered motion of internal degrees of freedom in fermionic quantum many-body systems (see, e.g., [1]). The width  $\Gamma$  is commonly explained to result from two contributions: direct particle emission from the initial one-particle one-hole (1p1h) excitations expressed by an escape width  $\Gamma^\dagger$  and coupling to more complex 2p2h and finally  $n$ pnh states leading to a spreading width  $\Gamma^\ddagger$  due to internal mixing (see, e.g., [2]). It is generally agreed that internal mixing occurs through a hierarchy of couplings (an assumption underlying all transport theories [3–5]) towards more and more complex degrees of freedom in the nucleus. Such a scheme implies the existence of lifetimes characteristic for each coupling step with corresponding energy scales ranging from the total width of the order of MeV to the width of compound-nuclear states of the order of eV.

While this picture is widely accepted, direct experimental evidence is scarce. Probably the best established example refers to the isoscalar giant quadrupole resonance (ISGQR) in the doubly-magic nucleus  $^{208}\text{Pb}$  where the comparison of high-resolution [ $\Delta E \approx 50$  keV full width at half maximum (FWHM)] measurements using inelastic electron and proton scattering showed that the observed cross section fluctuations are independent of the exciting probe [6] and thus are physical in nature. After early attempts with a doorway state model [7], novel analysis ideas have been presented recently. Signatures are, for example, the observation of multiple scales deduced from an entropy index method (EIM) [8] or a multifractal analysis of the fluctuating strength function

[9]. Such characteristic scales provide a unique way to test microscopic many-body theories. In the EIM, the information entropy is calculated by folding the measured cross section with a weight function  $\Psi_j(E) = \text{sign}(E_j - 1/2)\delta E$  which depends on the bin size  $\delta E$  for each spectral bin  $j$ . An application of the EIM to the present case is discussed in [10], where by comparison with second random-phase approximation (SRPA) calculations it could be demonstrated that the observed scales result from the first step of the coupling hierarchy, i.e., 1p1h to 2p2h states.

This very interesting result immediately raises several questions: Are the scales a global feature found in all nuclei or are they specific to the doubly-magic nucleus  $^{208}\text{Pb}$ ? Do the methods discussed in [8,9] provide unique results? What is the physical nature of the scales?

To explore these issues, a series of high-resolution ( $p, p'$ ) measurements was performed at the cyclotron of iThemba LABS, Somerset West, South Africa, using a K600 magnetic spectrometer. Data were taken for isotopically enriched (>95%) targets of  $^{58}\text{Ni}$ ,  $^{89}\text{Y}$ ,  $^{90}\text{Zr}$ ,  $^{120}\text{Sn}$ , and  $^{208}\text{Pb}$  with typical areal densities of several  $\text{mg}/\text{cm}^2$  and incident proton currents of 1–20 nA. The measured laboratory scattering angles of  $8^\circ$ – $10^\circ$  correspond to the maximum of  $\Delta L = 2$  angular distributions where the excitation of the ISGQR is enhanced. In the case of  $^{90}\text{Zr}$  and  $^{208}\text{Pb}$ , extended angle ranges ( $6^\circ$ – $14^\circ$ ) were measured in addition to study the possible influence of other multipoles on the analysis described below. These were found to be of minor importance. Using beam dispersion matching techniques, very good energy resolutions  $\Delta E \approx 35$ – $45$  keV (FWHM) could be achieved. Figure 1 shows

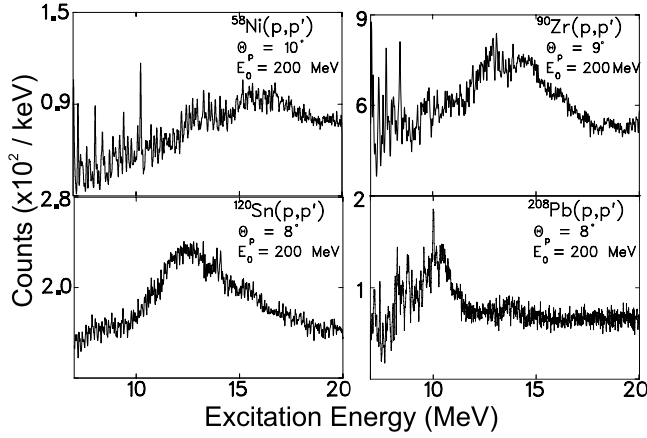


FIG. 1. Spectra of the  $(p, p')$  reaction at  $E_0 = 200$  MeV on  $^{58}\text{Ni}$ ,  $^{90}\text{Zr}$ ,  $^{190}\text{Sn}$ , and  $^{208}\text{Pb}$  with a typical energy resolution  $\Delta E \approx 40$  keV FWHM. The scattering angles were chosen to enhance the excitation of the ISGQR.

some examples of the measured spectra. Pronounced fine structure is visible over the excitation energy range of the ISGQR in all nuclei investigated.

For the extraction of characteristic scales in the fine structure wavelet analysis techniques, developed in signal theory [11], have been explored. By folding the original spectrum  $\sigma(E)$  with a chosen wavelet function  $\Psi$ , coefficients

$$C(E_x, \delta E) = \frac{1}{\sqrt{\delta E}} \int \sigma(E) \Psi\left(\frac{E_x - E}{\delta E}\right) dE \quad (1)$$

are obtained. The parameters (excitation energy  $E_x$  and bin size  $\delta E$ ) can be varied continuously or in discrete steps  $j$ , where  $\delta E = 2^j$ ,  $j = 1, 2, 3 \dots$ , and  $E_x = \delta E$ . Here, because of space limitations, the presentation of results is restricted to the continuous case and with the use of a specific wavelet function of the Morlet type consisting of a cosine function with a Gaussian envelope

$$\Psi(x) = \frac{1}{\sqrt{\pi}} \cos(kx) \exp\left(-\frac{x^2}{2}\right). \quad (2)$$

A value  $2\pi k = 5$  was found empirically to provide optimal properties in localizing the scales.

As an example, we discuss the case of  $^{208}\text{Pb}$  allowing direct comparison with previous analyses. The resulting two-dimensional correlation of the squares of the wavelet coefficients, Eq. (1), is displayed in Fig. 2. One apparent advantage of this method over those proposed in [8,9] is the ability to locate the excitation energy regions in the spectrum where a scale appears. In the present case, pronounced maxima extend over the region of the ISGQR bump at characteristic values of  $\delta E$ . The corresponding power spectrum, projected on the wavelet scale axis, allows to extract values of 40, 120, 440, 850, and 1500 keV. Here, the smallest scale is due to the experimental energy resolution of the spectrum while the large

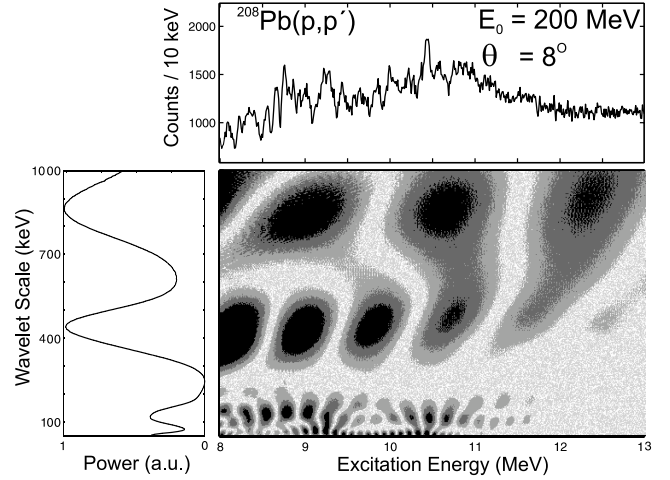


FIG. 2. Upper part: Spectrum of the  $^{208}\text{Pb}(p, p')$  reaction. Central part: Squares of the wavelet coefficients as a function of excitation energy and scale using a Morlet function, Eq. (2). Left part: Projection of the wavelet coefficients on the scale axis (power spectrum).

est one reflects the total width of the ISGQR (not shown in Fig. 2 because the scale axis is limited to 1 MeV for better visibility). It may be noted that these results are largely consistent with the EIM analysis [10]. However, an additional scale is observed at 850 keV which has been missed previously because of the limited resolution of the entropy index method.

A global analysis of all available experimental data reveals three classes of scales: all nuclei studied so far exhibit a scale around 100 keV (class I), two or three scales between about 100 keV and 1 MeV strongly varying from nucleus to nucleus (class II), and a scale of several MeV reflecting the total width of the resonance (class III).

For a theoretical interpretation of these findings we focus again on  $^{208}\text{Pb}$  because a variety of microscopic calculations including 2p2h states at different levels of approximation and using different effective interactions are available. The importance of complex degrees of freedom is stressed by the fact that RPA calculations of the ISGQR lead to a single collective state which does not produce any scales in the wavelet analysis at all. Strength functions calculated with SRPA [10], quasiparticle-phonon model (QPM) [12], extended time-dependent Hartree-Fock (ETDHF) [13], and an extended theory of finite Fermi systems (ETFFS) [14] are available. The predictions differ substantially, but when analyzed in the framework described above, characteristic scales are identified in all cases. A summary of the results is presented in Table I. Qualitatively, the features observed in the data are reproduced. All calculations show a class I and a class III scale. Furthermore, two scales in the intermediate energy range (class II) are consistently found but with considerably varying values, reflecting sensitivity to the chosen interactions and/or model spaces.

TABLE I. Characteristic scales (in keV) of the ISGQR in  $^{208}\text{Pb}$  extracted from the wavelet analysis of the experimental  $(p, p')$  spectrum and various calculations, labeled according to the classes discussed in the text.

Scale classes	I	II	III
Experiment	120	440 850	1500
SRPA [10]	80	240 700	1300
QPM [12]	80	510 820	1600
ETDHF [13]	120	230 840	1400
ETFFS [14]	130	310 570	2600

The success in reproducing at least the qualitative features of the characteristic scales clearly motivates attempts to extract their underlying physical nature from the models. As an example, we want to base our discussion on the QPM approach which provides a highly successful description of collective nuclear modes [15–17]. The comparison of the experimental  $^{208}\text{Pb}$  spectrum from Fig. 1 with the QPM prediction (upper l.h.s. of Fig. 3) for isoscalar  $E2$  strength indicates a slight underestimation of the fragmentation, but the scales visible in the experimental wavelet power spectrum are reproduced well (upper r.h.s. of Fig. 3).

An important mechanism contributing to the damping of the single-particle [18] as well as the collective re-

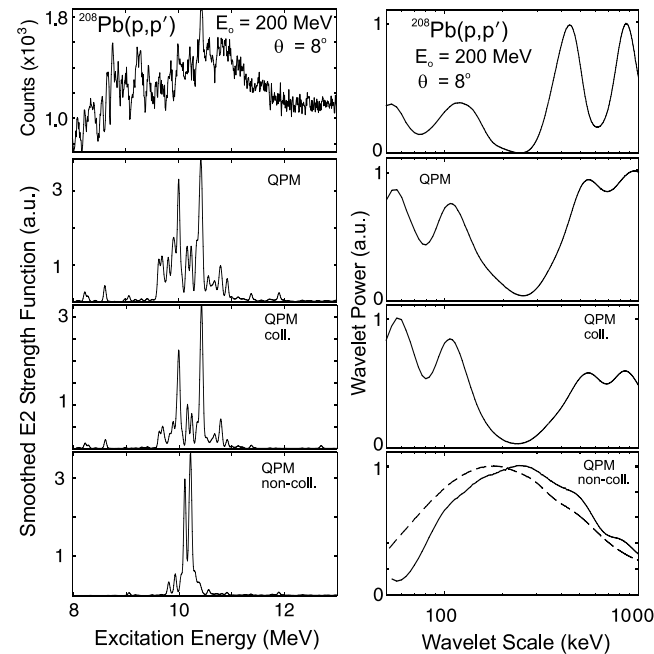


FIG. 3. Left panel: Experimental spectrum for  $^{208}\text{Pb}$ , QPM prediction of the ISGQR strength function, and its decomposition into a collective part due to the coupling to low-lying surface vibrations and a noncollective part due to the coupling to the background of  $2p2h$  states. Right panel: Corresponding wavelet power spectra (solid lines). The maxima indicate characteristic scales. The dashed line shows the result obtained for the stochastic coupling model described in the text.

sponse in heavy nuclei is the coupling to low-lying surface vibrations [1,19], called “collective” hereafter. On the other hand, significant contributions also come from mixing of the initial  $1p1h$  states with the large background of states with more complex wave functions, termed “noncollective.” The two contributions can be approximately disentangled within the QPM by investigating the properties of the coupling matrix elements  $V_{2ph}^{1ph}$  between the one- and two-phonon configurations. The probability  $P$  of finding a certain value of  $V_{2ph}^{1ph}$  is displayed as a histogram in Fig. 4 for the case of  $^{208}\text{Pb}$ . The distribution deviates appreciably from the Gaussian form (solid line in Fig. 4) expected for chaotic systems: one finds a strong overshoot of very small matrix elements and some enhancement at large values. Very similar features have been reported from the analysis of off-diagonal interaction matrix elements in shell-model calculations [20]. The excess of small matrix elements indicates that many two-phonon configurations contribute little to the fragmentation process. On the other hand, the large matrix elements have an appreciable effect and are due to the presence of soft collective modes.

For a separation of the collective and noncollective mechanisms as prescribed above, the two-phonon configurations are divided into two subspaces: (i) a large subspace with  $V_{2ph}^{1ph}$  following the Gaussian distribution (plus overshoot small matrix elements) and (ii) a small subspace with large  $V_{2ph}^{1ph}$  values above the Gaussian tails. Then the QPM Hamiltonian has been diagonalized in the one- plus (i) or (ii) two-phonon subspaces. The resulting  $E2$  strength functions are displayed on the lower l.h.s. of Fig. 3. It is obvious that the fragmentation is dominated by the collective mechanism. One should also keep in mind

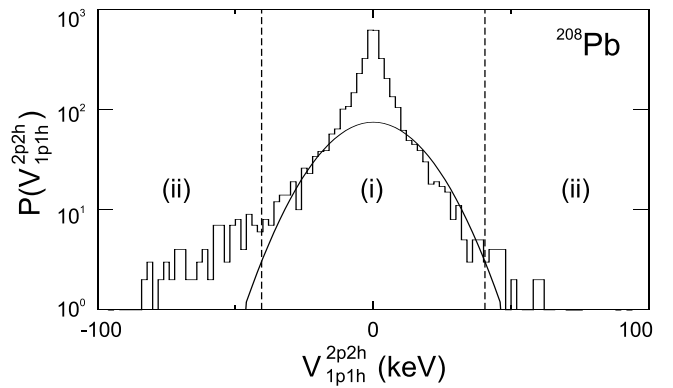


FIG. 4. Distribution of coupling matrix elements  $V_{2ph}^{1ph}$  between the one- and two-phonon configurations in the QPM calculation of the ISGQR strength function for  $^{208}\text{Pb}$ . The solid line denotes a Gaussian distribution expected for a chaotic system with a width in accordance with the QPM results. The dashed lines indicate the cutoff value of  $V_{2ph}^{1ph}$  between model spaces (i) and (ii) describing the contributions of the noncollective and the collective mechanisms, respectively, to the fine structure.

that the full calculation is not just the sum of the two contributions but interference terms may play a role. The corresponding wavelet power spectra are displayed on the lower r.h.s. of Fig. 3. The decomposition makes clear that all scales in the calculation are already present in the collective part while little indication of specific scales is found in the noncollective part. These findings are confirmed by a comparable analysis within the ETDHF model based on a perturbation approach [13].

The absence of pronounced scales in the noncollective part suggests a generic origin, i.e., a stochastic coupling to a “background” of complex states. Then, the level spacings and coupling matrix element distributions are described by the Gaussian orthogonal ensemble (GOE). In order to test this assumption, we have generated a GOE with the same Gaussian distribution of the matrix elements as found in the QPM calculation of  $^{208}\text{Pb}$ . After averaging over an ensemble of 20 random copies, the wavelet analysis leads to the power spectrum displayed in Fig. 3 as the dashed line. Indeed, the stochastic coupling model produces a large variety of scales which manifests itself in a broad distribution, exactly what is seen in the QPM results for the noncollective subspace (i). The slight shift of the maximum and the remnants of the scales at 510 and 820 keV visible in the QPM prediction can probably be traced back to the decomposition procedure. Rather than taking all matrix elements exceeding the Gaussian distribution at a given strength, one has to define a cutoff value indicated by the dashed lines in Fig. 4 below which all matrix elements are assumed to belong to subspace (i).

In conclusion, high-resolution inelastic proton scattering data on nuclei covering a wide mass range establish the fine structure of the ISGQR, first observed in  $^{208}\text{Pb}$ , as a global phenomenon. A novel method based on wavelet transforms is presented which allows the extraction of scales characterizing the fine structure. These are signatures of the coupling of collective  $1p1h$  states to low-lying surface vibrations. Thus, the present results provide direct experimental evidence for the doorway mechanism [1] being the dominant contribution—at least in heavy nuclei—to the spreading width  $\Gamma^\downarrow$ . On the other hand, the coupling to the background of complex states leads to a characteristic pattern in the wavelet analysis resulting from the stochastic nature of the process.

Despite the successful qualitative analysis, problems remain for a quantitative interpretation. A theoretical understanding of the strong model dependence of the predicted scales summarized in Table I is called for. Another open question is the role of the escape width, whose contribution becomes important for lighter nuclei. Experimental evidence for scales induced by the next level of complexity in the hierarchical coupling scheme would be of high interest. This may be possible by studying the  $\gamma$  decay of the ISGQR with arrays like GAMMASPHERE or EUROBALL. In the future, even

compound-nucleus scales may be accessible using attosecond-pulsed laser-electron interaction [21]. Finally, fine structure has been observed in other collective electric and magnetic modes [22], and the wavelet analysis presented here promises to be a unique tool to gain new insight into the damping process of giant resonances in general.

We are indebted to L. Conradie and the accelerator crew at iThemba LABS for providing excellent beams. We thank R.T. Newman and S. Mukherjee for their help in the data taking. Discussions with P.F. Bortignon, G. Cooper, H. Feldmeier, S. Galès, and R.G.T. Zegers are gratefully acknowledged. This work has been supported by the DFG under Contracts No. SFB 634 and No. 445 SUA-113/6/0-1, and by the South African NRF.

---

\*Email address: vnc@ikp.tu-darmstadt.de

†Permanent address: Bogoliubov Laboratory for Theoretical Physics, JINR, Dubna, Russia.

- [1] P.F. Bortignon, A. Bracco, and R.A. Broglia, *Giant Resonances: Nuclear Structure at Finite Temperature* (Harwood Academic, Amsterdam, 1998).
- [2] M.N. Harakeh and A. van der Woude, *Giant Resonances: Fundamental High-Frequency Modes of Nuclear Excitation* (Oxford University, Oxford, 2000).
- [3] W. Cassing and U. Mosel, *Prog. Part. Nucl. Phys.* **25**, 235 (1990).
- [4] P.-G. Reinhard and C. Toepffer, *Int. J. Mod. Phys. E* **3**, 435 (1994).
- [5] Y. Abe *et al.*, *Phys. Rep.* **275**, 49 (1996).
- [6] S. Kamedzhiev *et al.*, *Phys. Rev. C* **55**, 2101 (1997).
- [7] J. Winchenbach *et al.*, *Nucl. Phys.* **A410**, 237 (1983).
- [8] D. Lacroix and P. Chomaz, *Phys. Rev. C* **60**, 064307 (1999).
- [9] H. Aiba and M. Matsuo, *Phys. Rev. C* **60**, 034307 (1999); H. Aiba *et al.*, *Phys. Rev. C* **68**, 054316 (2003).
- [10] D. Lacroix *et al.*, *Phys. Lett. B* **479**, 15 (2000).
- [11] *Wavelets and Their Applications*, edited by R. Coifman (Jones and Barlett, Boston, 1992).
- [12] C.A. Bertulani and V. Yu. Ponomarev, *Phys. Rep.* **321**, 139 (1999).
- [13] D. Lacroix *et al.*, *Phys. Rev. C* **63**, 064305 (2001).
- [14] S. Kamedzhiev *et al.*, *Phys. Rep.* **393**, 1 (2004).
- [15] V. Yu. Ponomarev and P. von Neumann-Cosel, *Phys. Rev. Lett.* **82**, 501 (1999).
- [16] B. Reitz *et al.*, *Phys. Lett. B* **532**, 179 (2002).
- [17] N. Ryezayeva *et al.*, *Phys. Rev. Lett.* **89**, 272502 (2002).
- [18] S. Galès *et al.*, *Phys. Rep.* **166**, 125 (1988).
- [19] G. F. Bertsch *et al.*, *Rev. Mod. Phys.* **55**, 287 (1983).
- [20] V. Zelevinsky *et al.*, *Phys. Rep.* **276**, 85 (1996).
- [21] N. Milosevic *et al.*, *Phys. Rev. Lett.* **92**, 013002 (2004).
- [22] A. Richter, *Nucl. Phys.* **A731**, 59 (2004); P. von Neumann-Cosel, *Proceedings of the 32nd International Workshop on Gross Properties of Nuclei and Nuclear Excitations*, edited by M. Buballa *et al.* (GSI, Darmstadt, 2004), p. 189.